Exploring the human fetal brain network with diffusion MRI and graph theory

Virendra Mishra[1], Ni Shu[2], Lina Chalak[3], Nancy Rollins[4], Cathy Halovanic[5], Yong He[2], and Hao Huang[1]

[1]*Advanced Imaging Research Center, University of Texas Southwestern Medical Center, Dallas, TX, United States,* [2]*State Key Laboratory of Cognitive Neuroscience and Learning, Beijing Normal University, Beijing, Beijing, China,* [3]*Department of Pediatrics, University of Texas Southwestern Medical Center, Dallas, TX, United States,* [4]*Department of Radiology, University of Texas Southwestern Medical Center, Dallas, TX, United States,* [5]*Children's Medical Center of Dallas, Dallas, TX, United States*

Target audience: The clinicians, MR physicists and neuroscientists interested in understanding prenatal or fetal brain development with high resolution DTI and graph theory.

Introduction and Purpose: The proper "wiring" of the developmental human brain plays a key role in developing normal mental brain functions. Network abnormalities have been found to be associated with developmental cognitive brain disorders such as mental retardation, autism, schizophrenia, bipolar disorder and language impairment [e.g. 1,2]. Characterizing the normal prenatal brain network development will not only expand our understanding of formation of functionally significant brain circuits, but also shed light on understanding the abnormal network development associated with child mental health. The axonal connectivity during prenatal brain development undergoes dramatic structural changes causing significant variations of brain network properties. However, without a cortical node definition and limited studies on white matter axonal connectivity of the fetal brain [3-6], prenatal brain network development has not been characterized in the literature. DTI based tractography allows us to noninvasively probe the structural connectivity. The midpoint of prenatal development (20 weeks of gestation or 20wg) to birth is a landmark time point of fetal brain development. In this study, high resolution DTI data of *ex vivo* fetal brains at 20 wg and *in vivo* neonatal brain at 40 wg (term) were acquired. Graph theory analysis was conducted with the brain nodes parcellated from a template free algorithm [7] and edges quantified based on DTI tractography.

Methods:

DTI acquisition of 20wg fetal brain: 4.7T Bruker scanner was used to acquire data from 10 postmortem fetal brain samples at around 20 wg. A 3D multiple spin echo DTI sequence was used. The diffusion weighted images (DWI) parameters were: b-value=1000s/mm^{2}T, resolution= 0.29x0.29x0.29mm^3. *DTI acquisition of 40wg neonate brain:* A Philips 3T scanner was used to acquire *in vivo* DTI from 20 neonates. A single-shot EPI sequence with SENSE parallel imaging scheme (reduction factor =2.5) was used. DWI parameters were: b-value=1000 sec/mm^2, resolution= 2x2x2mm^3, repetition=2. *Cortical parcellation for network node definition:* Due to the lack of anatomical landmarks on 20 wg brain, a template-free parcellation scheme [7] was applied to parcellate each brain into 80 different regions with similar size. The segmented nodes were constrained to be consistent across the hemispheres for each brain and consistent across the brains of different subjects. *DTI tractography for network edge generation:* With each of the 80 parcellated nodes as seeds, deterministic tracking was performed using Trackvis [8]. A filtering algorithm was applied to keep only tracts connecting two different nodes and an 80x80 weighted connectivity matrix was established for each subject. The weights of the network edge were defined from the relative fiber volume connecting two of 80 nodes. Fig.1 shows orientation-encoded DTI colormap, whole brain fibers derived from DTI tractography and cortical nodes of a typical 20wg and 40wg fetal brain. The nodes and connectivity fibers were used for establishing the network. *Network analysis with graph theory:* With different edge weight thresholds, strength, cost efficiency and small-worldness were calculated using GRETNA toolbox [9] from 6 brains in each age group. The statistical comparison between the two groups was analyzed using student t-test.

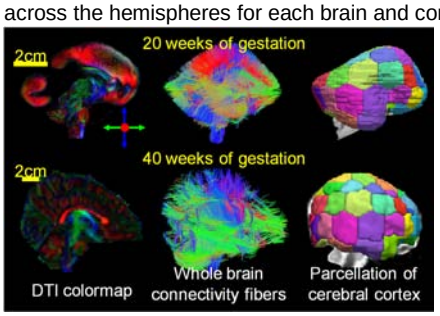

Fig. 1: Sagittal views of orientation-encoded DTI colormap, whole brain connectivity fibers and parcellation of the cortical nodes of a 20wg (upper panel) and 40wg (lower panel) fetal brain.

Results: *All brain fibers filtered at different lengths:* Fig. 2 demonstrates the all brain fibers filtered at different lengths, namely a certain portion of the brain size L, for a typical 20wg and 40wg fetal brain. It shows the correspondent white matter connections by gradually removing different levels of short fibers. From left to right, fibers with lengths less than 0 (no fiber removed), 1/8L, 1/4L and 3/8L were removed. It is clear that even fetal brain at 20 weeks is rich of fibers. However, the long fibers at 20 weeks are mostly projection fibers mapping from cortex to spinal cord (Fig. 2d). There are no long fibers initiated from occipital lobe at 20 weeks while there are quite a few fibers from occipital lobe projecting to distal frontal and temporal lobe at 40 weeks. The most apparent differences of the white matter connectivity between the brain at 20 weeks and the brain at 40 weeks are the long association tracts connecting occipital and frontal lobes at 40 weeks. *Comparisons of averaged connectivity matrix, cost efficiency, strength and small-worldness of two age groups:* As shown in Fig. 3, the averaged connectivity matrix of 40wg group shows stronger yet sparser nonzero connectivity, compared to that of 20wg group. Cost efficiency of 40wg brain is significantly higher for lower thresholds of edge weight, indicating that abundant short fibers in 20wg brains reduce the cost efficiency. Network strength of 40wg brains is higher than that of 20wg brains, yet not significantly at any threshold. However, the integration of the strength of 40wg brain across all the thresholds is significantly higher than that of 20wg brain ($p<0.001$). Interestingly, small worldness property already exists even for 20wg fetal brain (small-worldness>1). It also exists for 40wg brain.

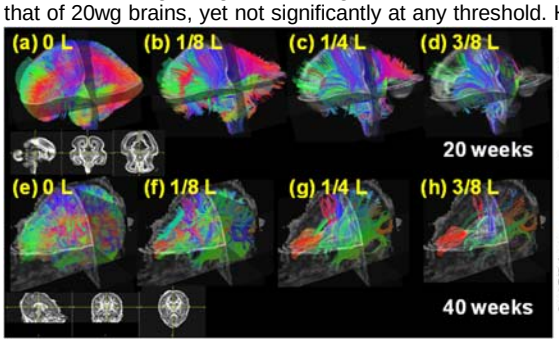

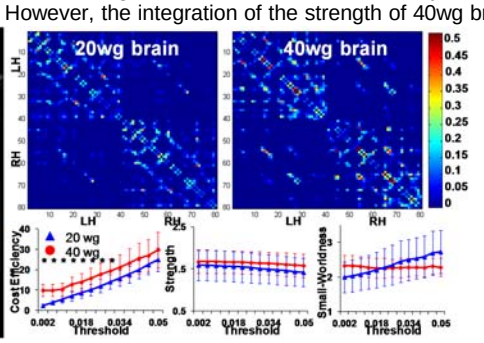

Fig. 2 (left): White matter connectivity differences between a 20 wg brain and a 40 wg brain by comparing all white matter fibers filtered with the same relative lengths.

Fig. 3 (right): Averaged connectivity matrices (upper panel) and comparisons of cost efficiency, strength and small-worldness at different edge weight thresholds (lower panel) for a group of 20wg brains and a group of 40wg brains. Asterisks indicate p less than 0.05. LH/RH: Left/right hemisphere.

Discussion and Conclusion: In this study, the formation of a more cost-efficient and stronger network from 20wg to 40wg was revealed. The process is characterized with reducing short fibers and increasing long fibers. It may seem counterintuitive that the small-worldness property already exists in 20wg brain. However, previous studies [e.g. 4-6] show that some association fibers, including uncinate, inferior longitudinal and inferior fronto-occipital fasciculus, become apparent in 20wg brain. In addition, ganglionic eminence is prominent and connects different brain regions at this time point. The network property changes found in our study could be underlined by significant growth of major long association white matter tracts with increased myelination and concurrent pruning of small fibers during prenatal brain development. Analysis with more brain data is underway. Inclusion of more samples may reduce the standard deviation and demonstrate the significant difference of network strength and other network measures.

References: [1] Power et al (2010) Neuron 67: 735-748. [2] Bullmore and Sporns (2009) Nature Rev Neurosci 10: 186-198. [3] Takahashi et al (2012) Cereb. Cortex 22:455-464. [4] Huang et al (2009) J. Neurosci. 29:4263-4273. [5] Vasung et.al (2010) J. Anat. 217:400-417. [6] Kostovic et.al (2006) Semin. Fetal. Neonatal. Med. 11:415-422. [7] Tymofiyeva et al (2012) PLoS ONE 7: e31029. 8) Wang et.al (2007) ISMRM 5720 9) Wang et al (2012) PLoS ONE 6: e21976. **Acknowledgement**: This study is sponsored by NIH MH092535 and NIH MH092535-S1.